# EFFECTIVENESS OF THE SPATIAL ACCELERATION MODULUS FOR ROLLING ELEMENTS BEARING FAULT DETECTION

Michele COTOGNO[1], Marco COCCONCELLI[2], Riccardo RUBINI[3]

[1]University of Modena and Reggio Emilia, Department of Science and Engineering Methods, Via Amendola, 2 – Morselli Building, 42122 Reggio Emilia, Italy
michele.cotogno@gmail.com
[2]University of Modena and Reggio Emilia, Department of Science and Engineering Methods, Via Amendola, 2 – Morselli Building, 42122 Reggio Emilia, Italy
marco.cocconcelli@unimore.it
[3]University of Modena and Reggio Emilia, Department of Science and Engineering Methods, Via Amendola, 2 – Morselli Building, 42122 Reggio Emilia, Italy
riccardo.rubini@unimore.it

Summary

Rolling Elements Bearing (REB) condition monitoring is mainly based on the analysis of acceleration (vibration) signal in the load direction. This is one of the three components of the acceleration vector in 3D space: the main idea of this paper is the recovery of additional fault information from the other two acceleration vector components by combining them to obtain the modulus of the spatial acceleration (SAM) vector. The REB diagnostic performances of the SAM are investigated and compared to the load direction of vibration by means a rough estimator of the "Signal-to-Noise" Ratio and the Spectral Kurtosis. The SAM provides a higher SNR than the single load direction. Finally, Spectral Kurtosis driven Envelope analysis is performed for further comparison of the two signals: its results highlight that demodulation of the SAM isn't strictly necessary to extract the fault features, which are already available in the raw signal spectrum.

Keywords: Rolling Element Bearing, Diagnostic, Spatial Acceleration Modulus, SAM, SNR, Spectral Kurtosis, Envelope Analysis.

## 1 Introduction

Rolling Elements Bearing (REB) condition monitoring is mostly based on the analysis of the vibration signal [1,2]. This is typically obtained from an accelerometer which measures the intensity of vibration (i.e.: acceleration) along the load direction. Many signal processing techniques are available for the REB fault features extraction: they mainly deal with the fact that the measured vibration signal is the sum of different components (mechanical/electrical noise, the effect of vibration path from the REB to the sensor, vibrations coming from other moving parts in the machinery, etc.) which mask the fault signature. Additional fault information may be recovered from all the three acceleration components by analyzing the modulus of the spatial acceleration vector (SAM, [9]). In particular, it is supposed that one effect of the vibration path could be the spread of the signal of interest along other axes of acceleration rather than preserving it in the load direction only. Indeed, a faulty bearing produces a series of vibration pulses that excite all the vibration modes of the system, including the transversal modes (with respect to the load direction): thus traces of this pulse series could also be embedded in vibration data along the non-load directions. The SAM should embody this extra information, and it's obtained for every instant $t$ by the following Eq. 1:

$$SAM(t) = \sqrt{(x(t)-\mu_x)^2 + (y(t)-\mu_y)^2 + (z(t)-\mu_z)^2} \tag{1}$$

where $x(t)$, $y(t)$ and $z(t)$ are the acceleration vector projections acquired by the triaxial accelerometer at time $t$, and $\mu_x$, $\mu_y$ and $\mu_z$ are the temporal averages of the respective axis. In this paper the SAM is compared with the acceleration signal along the load axis (i.e.: the classically analyzed signal in REB condition monitoring) in case of loaded and unloaded bearing, healthy and faulty bearing. Equation 1 highlights that the SAM will exhibit larger (and non-negative) values than any single axis of acceleration, and this consideration can be extended also to the respective amplitude spectra. Consequently, a direct quantitative comparison between the SAM and any single acceleration axis (and between their spectra) can't be completely truthful. In order to overcome this issue, some attempts of estimation of the Signal-to-Noise Ratio (SNR) are performed on real REB data and reported in the next sections.

## 2 SNR estimation: unloaded bearing

The bearing used in this series of experiments is SKF1205ETN9. The data are recorded at 25 kHz sampling frequency by a PCB356A01 triaxial accelerometer, from healthy and faulty bearing at five different bearing rotation speed ($f_r$ = 15, 25, 35, 45 and 60 Hz). The artificial fault is made on the outer race. The only load applied is weight, directed along the $y$ axis of the accelerometer: this axis of vibration is the classically analyzed in REB condition monitoring and is therefore used for performance comparison with the SAM. The analysis is performed on the raw data in order to evaluate the amount of information spontaneously embodied in the signals. In Fig. 1a (healthy bearing) and Fig. 1b (faulty bearing) extracts of the vibration data along the load axis are reported and compared to the correspondent time sections of the SAM (Fig. 1c – 1d).

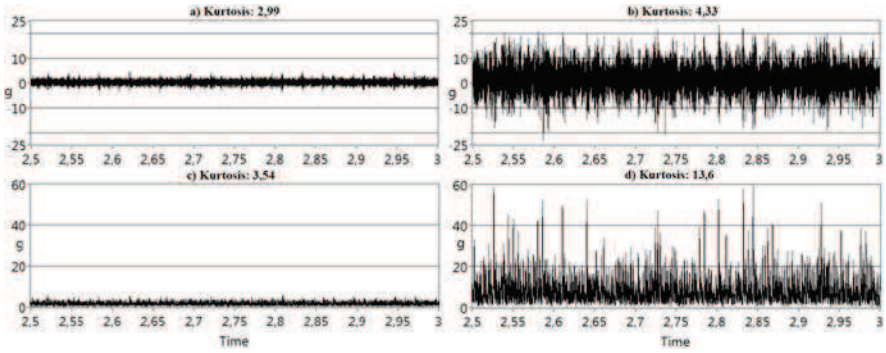


Fig. 1. Time sections of vibration data: a) load axis, healthy bearing; b) load axis, faulty bearing; c) SAM, healthy bearing; d) SAM, faulty bearing

Figure 1 confirms that the amplitude of the signal is larger for the SAM. Moreover, it seems to have a more "spiky" nature than the load axis, particularly in presence of a fault (Fig. 1d): this observation is acknowledged by the global Kurtosis index (4,33 for the load axis and 13,6 for the SAM in case of faulty bearing); i.e., the SAM is representing the pulses of vibration in a clearer manner.

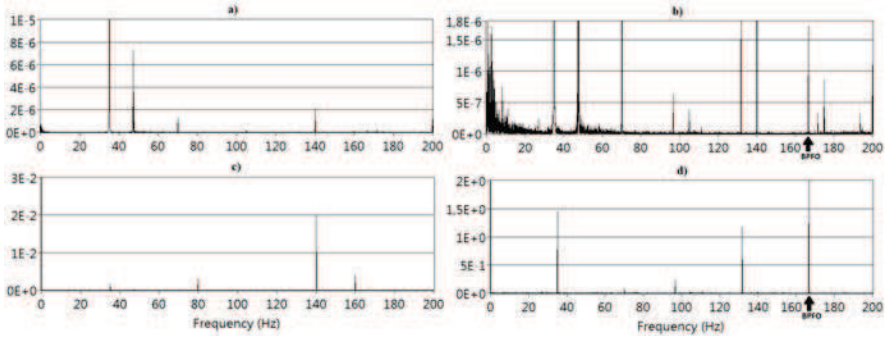


Fig. 2. Autospectra of: a) load axis, healthy bearing; b) load axis, faulty bearing; c) SAM, healthy bearing; d) SAM, faulty bearing. ($f_r$ = 35Hz, BPFO = 167Hz). The Y scales are different in order to highlight the amplitudes of interest more clearly

In Figure 2 the autospectra of the load axis and the SAM are reported in case of healthy bearing (resp. Fig. 2a and 2c) and in case of outer race fault (resp. Fig 2b and 2d): in these cases the bearing rotation speed ($f_r$) is 35Hz giving a theoretical Ball Pass Frequency on Outer Race (BPFO) of 167Hz. Figure 3 is equivalent to Figure 2 except for $f_r$ of 45Hz (theoretical BPFO of 214,7Hz).

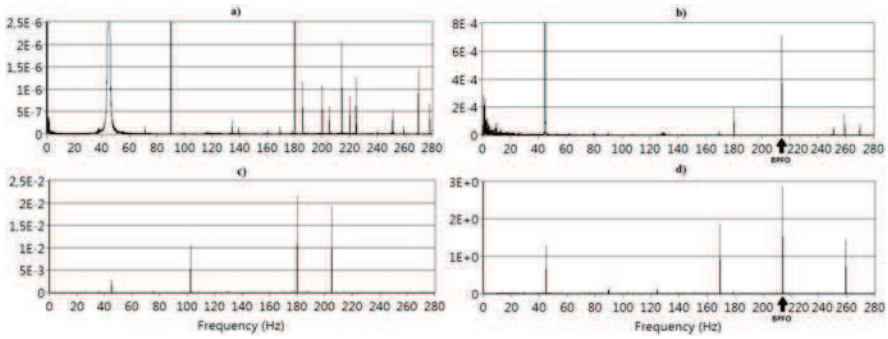


Fig. 3. Autospectra of a) load axis, healthy bearing; b) load axis, faulty bearing; c) SAM, healthy bearing; d) SAM, faulty bearing. ($f_r$ = 45Hz, BPFO = 214,7Hz). The Y scales are different in order to highlight the amplitudes of interest more clearly

As expected, the SAM spectrum is higher (usually 3 order of magnitude) than the load axis spectrum, thus hindering a direct spectra comparison. There are slight differences in the frequency position of the main spectrum peaks, probably because of the extra information gathered from the additional axes of vibration. In general, for the SAM the authors observe a "cleaner" and more communicative spectrum, in particular in case of a healthy bearing. In case of faulty bearing the SAM spectrum is dominated by the BPFO line, while the same isn't for the load axis spectrum (e.g.: Fig. 2). In order to perform a more meaningful comparison between the two signals, the "Signal-to-Noise" Ratio (SNR) is approximated by the $SNR_A$ estimator (Eq. 2): $SNR_A$ comes from the pragmatic definition of "signal" as the power in the BPFO ± 1% frequency band and "noise" as the mean spectrum power. The SAM exhibits higher $SNR_A$ than the load axis in all the experiments conducted (Table 1). The SAM $SNR_A$ increases when the fault is introduced except in case of high speeds (45 and 60Hz), where it decreases; this behavior is almost the exact opposite of the load axis $SNR_A$ (which exhibits also larger variations). This could be explained by the larger energetic content of the vibration signals at higher speeds which increases the denominator in Eq. 2, thus lowering the SAM $SNR_A$ indicator; in contrast, the load axis $SNR_A$ increases probably because at higher speeds its BPFO line shows a larger amplitude (Fig. 3b with respect to Fig. 2b) thus increasing the numerator in Eq. 2. The sum of these two effects and the slightly different nature of the two signals could explain the $SNR_A$ trends highlighted in Table 1. $SNR_A$ values are interpreted by the authors as a symptom of the SAM actually embodying more information or making it more readable than the load axis.

$$SNR_A = \frac{\text{power in the BPFO} \pm 1\% \text{ frequency band}}{\text{mean spectrum power}} \tag{2}$$

Table 1. Estimates of the Signal-to-Noise Ratio.

| | | $SNR_A$ (dB) | |
|---|---|---|---|
| $f_r$ (Hz) | Signal | Healthy bearing | Faulty bearing |
| 15 | Load axis | 8,9 | 0,4 |
| | SAM | 49,7 | 51,4 |
| 25 | Load axis | -9,7 | -12,2 |
| | SAM | 38,2 | 43,9 |
| 35 | Load axis | -9,8 | -18,5 |
| | SAM | 40,8 | 41,7 |
| 45 | Load axis | 1,4 | -13,5 |
| | SAM | 43,9 | 40,8 |
| 60 | Load axis | 0,8 | 2,5 |
| | SAM | 43,7 | 34,1 |

A more refined way to estimate the SNR is represented by the Spectral Kurtosis (SK) [3,4], a useful tool in condition monitoring [5] that can be used in REB diagnostics to find the optimum frequency band for the signal filtering prior to the Envelope analysis [2,6,7]. In [4] it is revealed that the SK is proportional to the square of the Wiener filter $W(f)$, which is defined by the following Eq. 3:

$$W(f) = \frac{1}{1+\rho(f)} \tag{3}$$

where $\rho(f)$ is the "Noise-to-Signal" Ratio, i.e. the inverse of the SNR. "Signal" here is interpreted as "randomly occurring pulses of random amplitude" [4] which is a model that has proven its effective-

ness in describing the vibration signal of a faulty REB. Thus, larger SK values are related to larger SNR of the data. In this paper, the SK is obtained by the following formula (Eq. 4), which is an unbiased STFT-based SK estimator proposed in [8]:

$$SK(f)=\frac{M}{M-1}\left[\frac{(M+1)\sum_{i=1}^{M}\left|X_i(f)\right|^4}{\left(\sum_{i=1}^{M}\left|X_i(f)\right|^2\right)^2}-2\right] \tag{4}$$

where $M$ is the number of non-overlapping blocks of the STFT and $X_i(f)$ is the DFT of the $i^{th}$ block of data. As highlighted in [4], the STFT block length (i.e.: the STFT window length, $N_w$ in the rest of this paper) must be set to have a temporal duration lower than the expected mean time between impacts (i.e.: BPFO) in order to get consistent results: this yields $N_w = 128$ samples in case BPFO = 167Hz and $N_w = 64$ samples in case BPFO = 214,7Hz. In Figure 4 the SK for these two experiments are reported.

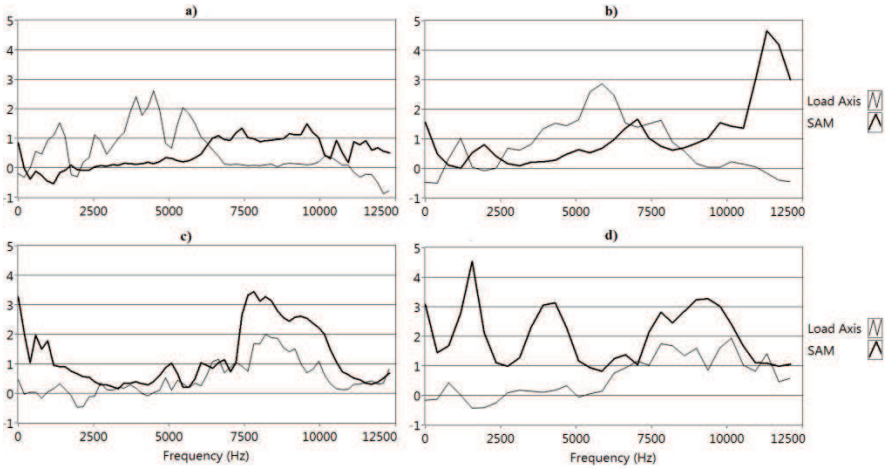


Fig. 4. Spectral Kurtosis of load axis and SAM; a) healthy bearing, $f_r = 35$Hz; b) healthy bearing, $f_r = 45$Hz; c) faulty bearing, $f_r = 35$Hz; d) faulty bearing, $f_r = 45$Hz

Fig. 4 shows that in case of healthy bearing (Fig. 4a and 4b) the SK of the SAM is lower (and closer to zero) than the SK of the load axis, and it increases more decisively when a fault is present (Fig. 4c and 4d, where the SAM SK graph is always over the load axis SK). In absence of the fault, the SAM SK overcomes the load axis SK in the 6,5 ÷ 12,5kHz (when $f_r = 35$Hz, Fig. 4a) and in the 8 ÷ 12,5kHz (when $f_r = 45$Hz, Fig. 4b) frequency bands. Zero-valued SK indicates that the signal is more similar to Gaussian noise rather than a series of transients, while the presence of the latter is highlighted by higher SK values: thus, the SAM SK is communicating more explicitly the existence of a fault. The frequency bands with higher Kurtosis indicated by the two SK are similar when the fault is present, and correspond to a system resonance band (approximately 7,5 ÷ 9,5kHz). It's notable that in the majority of the experiments the SAM SK exhibits the highest values also in the low frequency zone (i.e.: near the DC component), thus communicating that demodulation isn't strictly necessary to extract the fault signature from the SAM. This is in accord with the raw signals spectra comparison (Fig. 2, Fig. 3 and Table 1). These considerations about the SAM SK seem to confirm the higher SNR of the SAM than the load axis in case of unloaded bearing: in the next section the same study is performed and reported in case of loaded bearings.

## 3 SNR estimation: loaded bearing

In this series of experiments two damaged bearings had been used, these being a very worn SKF1205ETN9 and a KBC6205Z, both with an artificial outer race fault: the goal of this test was to investigate if the SAM performances are caused by the absence of a load applied to the REB. Indeed, the acquisition chain remained the same of the previous series of experiments (including the sampling frequency of 25kHz) but in this case two different radial loads of 589 N and 1178 N had been applied to the bearings; the REB speeds in this series of tests were 15, 25, 35, 45, and 53Hz. In Fig. 5 (SKF running at $f_r = 35$Hz – load 589 N) and Fig. 6 (KBC running at $f_r = 25$Hz – load 1178 N) the raw spectra of the load axis and the SAM are reported: also in case of loaded bearing, it can be observed that the SAM spectrum is much more "clean" and it's dominated by the BPFO, in contrast with the load axis spectrum where the BPFO is almost hidden. Generally, the features of the two spectra are those already observed in the previous section, thus indicating that the SAM appears very significant and communicative from the diagnostic point of view.

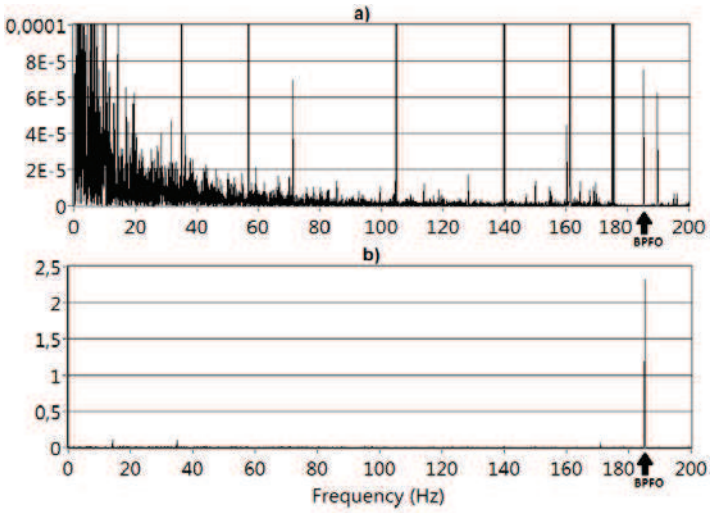


Fig. 5. Autospectra of a) load axis and b) SAM of the faulty SKF bearing running at $f_r$ = 35Hz (BPFO = 183,9 Hz) with 589 N of load applied.

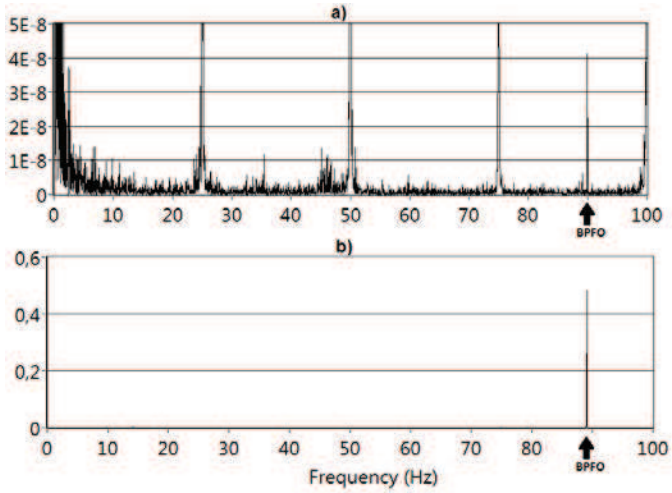


Fig. 6. Autospectra of a) load axis and b) SAM of the faulty KBC bearing running at $f_r$ = 25Hz (BPFO = 89,6 Hz) with 1178 N of load applied

The values of $SNR_A$ and $SNR_{CF}$ are reported in Table 2 and Table 3 (respectively: SKF and KBC bearing): these are calculated again from the raw vibration signals in order to evaluate their native information content.

Table 2. Values of $SNR_A$ for radial loaded SKF1205ETN9 bearing.

| | | $SNR_A$ (dB) | |
|---|---|---|---|
| $f_r$ (Hz) | Signal | load 589 N | load 1178 N |
| 15 | Load axis | -14,98 | 3,77 |
| | SAM | 40,29 | 37,13 |
| 25 | Load axis | 1,26 | -8,49 |
| | SAM | 37,62 | 35,59 |
| 35 | Load axis | -6,94 | -9,30 |
| | SAM | 36,64 | 34,48 |
| 45 | Load axis | 5,98 | -4,80 |
| | SAM | 34,89 | 33,60 |
| 53 | Load axis | 17,81 | 10,56 |
| | SAM | 33,77 | 33,30 |

Table 3. Values of $SNR_A$ for radial loaded KBC6205Z bearing.

| | | $SNR_A$ (dB) | |
|---|---|---|---|
| $f_r$ (Hz) | Signal | load 589 N | load 1178 N |
| 15 | Load axis | -1,28 | -11,88 |
| | SAM | 41,72 | 44,48 |
| 25 | Load axis | -6,72 | -11,66 |
| | SAM | 43,17 | 46,90 |
| 35 | Load axis | 7,85 | -0,81 |
| | SAM | 24,32 | 44,40 |
| 45 | Load axis | 10,72 | 15,39 |
| | SAM | 20,10 | 19,93 |
| 53 | Load axis | 5,98 | -1,68 |
| | SAM | 23,52 | 31,88 |

From Tables 2 and 3 it can be seen that the SAM exhibit higher SNR also in case of loaded bearings in all the trials. These SNR approximations confirm the observations made on the direct comparison of the spectra: the SAM represent the frequencies of

interest more clearly than the load axis also in case of loaded bearing. The Spectral Kurtosis of the two signals is reported in Fig. 7 in case of KBC bearing running at $f_r = 25$Hz under 1178 N of radial load. The SK of the SAM reaches its maximum at frequencies lower than the load axis SK, and the maximum value is greater for the SAM. Thus the SK indicates a better SNR for the SAM, but the difference between the SK of the two signals is less evident than in case of unloaded bearing (Fig. 4). This behavior of the SK is shared by the majority of the trials concerning loaded bearings, thus it suggests that it isn't necessary to demodulate the SAM to obtain diagnostic information of the bearing – an observation concordant with the direct spectra comparison and the $SNR_A$ values.

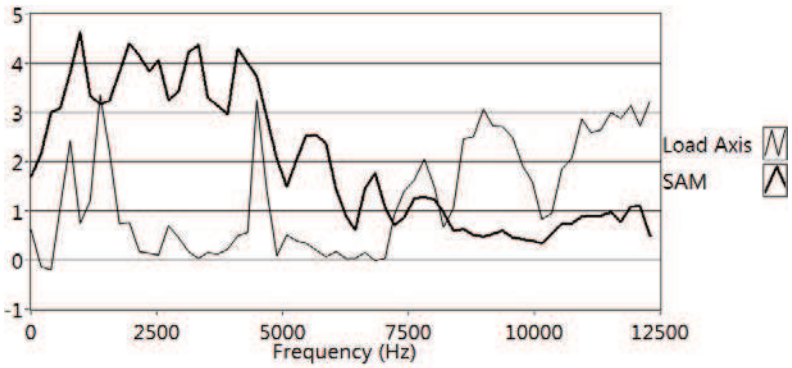


Fig. 7. Spectral Kurtosis of load axis and SAM; KBC bearing, $f_r = 25$Hz, load is 1178 N

## 4 Envelope Analysis

Envelope Analysis [1,2,7] is the benchmark signal processing tool for REB diagnostics. It performs a demodulation of the bandpass filtered signal. In this paper the filtering band is selected as the band in which the Spectral Kurtosis is maximized. The selected bands for the unloaded SKF bearing in case of $f_r = 35$Hz are 7,7 ÷ 8,8kHz for the load axis and 7,5 ÷ 8,5kHz for the SAM; in case of $f_r = 45$Hz they are 9,5 ÷ 10,5kHz for the load axis and 900 ÷ 1900Hz for the SAM. In Fig. 8 the Envelope spectra of the load axis and SAM are reported for the case of faulty unloaded SKF bearing rotating at $f_r = 35$Hz.

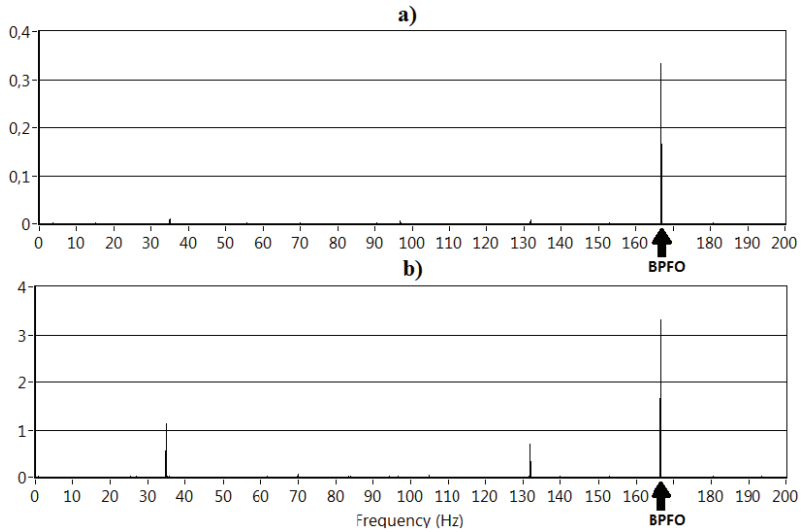


Fig. 8. Envelope Spectra of a) load axis and b) SAM for the unloaded SKF1205ETN9 bearing ($f_r = 35$Hz, BPFO = 167Hz)

It can be seen that the Envelope spectra of the SAM exhibit larger values, highlighting almost the same frequencies of the load axis. The dominating frequencies is the BPFO (167Hz) for both signals, but other notable frequencies (e.g.: the $f_r = 35$Hz frequency) exhibit higher magnitude in the SAM Envelope spectrum. This is about one order of magnitude higher than the load axis at those frequencies, while the average difference between the autospectra of the two signals is about 3 orders of magnitude (these considerations are valid for all the experiments). The BPFO magnitude in the SAM Envelope spectrum is about two times the correspondent magnitude in the raw SAM spectrum (respectively, 3,1 and 1,7); in contrast, the BPFO magnitude of the load axis Envelope spectra is about one million times the correspondent magnitude in the raw spectra (respectively, 0,3 and $1{,}75 \cdot 10^{-6}$).

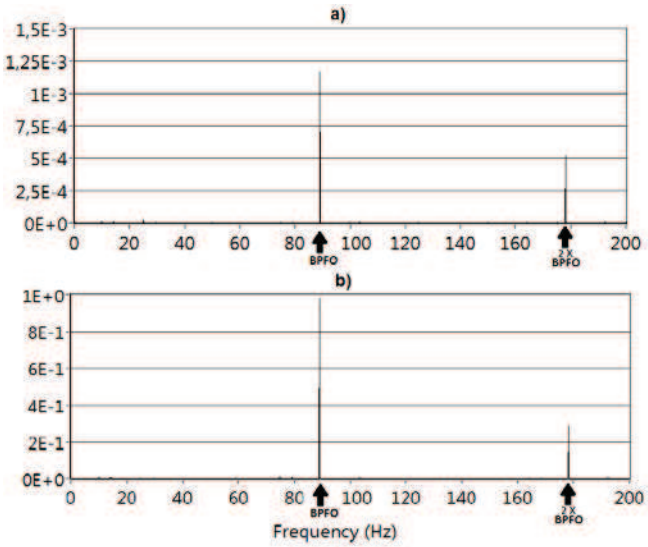


Fig. 9. Envelope Spectra of a) load axis and b) SAM for the KBC6205Z bearing (radial load of 1178 N, $f_r$ = 25Hz, BPFO = 89.6 Hz)

In Fig. 9 the Envelope spectra of the SAM and load axis are reported in case of loaded KBC bearing running at $f_r$ = 25Hz: the filtering band used for demodulation are 8.6 ÷ 9.6 kHz for the load axis and 0.6 ÷ 1.3 kHz for the SAM (i.e.: those with the maximum SK). The features of the Envelope spectra in case of loaded bearing are the same highlighted for the unloaded bearing: both spectra are dominated by the BPFO line but its amplitude is greater for the SAM. The demodulation permits to extract the information of interest from the load axis signal (its BPFO amplitude passes from $4.3 \cdot 10^{-8}$ to $1.16 \cdot 10^{-3}$, resp. Fig. 6a and Fig. 9a) while its action isn't so dramatic for the SAM (its BPFO amplitude passes from 0.5 to 1, resp. Fig. 6b and Fig. 9b), thus practically repeating the behavior highlighted in case of unloaded bearing. This observation confirms the indication of the Spectral Kurtosis of presence of high SNR in the low frequency zone of the SAM spectrum, signifying that demodulation isn't necessary for the SAM for the fault signature extraction.

## 5 Conclusions

In this paper the modulus of the spatial acceleration vector (SAM) is presented as a starting signal for rolling element bearings (REB) condition monitoring. Concerning the diagnostic capability, the SAM is compared to the acceleration component directed along the load axis, which is the classical analyzed signal in REB diagnostics. The comparison is performed on real raw REB data to evaluate the information spontaneously embedded in the signals: the data comes from two different bearings, encompassing the healthy and faulty, loaded and unloaded bearing conditions. Given the native amplitude difference between the two signals and their spectra (i.e., about three orders of magnitude), a rough approximation of the Signal-to-Noise Ratio is used to compare them - $SNR_A$ - which indicates always a higher SNR for the SAM. This is confirmed also by the Spectral Kurtosis (SK) analysis: higher SK is related to higher SNR and the SAM exhibit greater SK values in case of faulty bearing. Finally, Envelope analysis is performed and it also indicates a superior diagnostic capability of the SAM: its Envelope spectrum is generally one order of magnitude higher than the load axis Envelope spectrum. A comparison between the BPFO magnitude in the SAM Envelope spectrum and its correspondent in the raw SAM spectrum confirms that demodulation isn't necessary to extract the fault features, as indicated previously by the SK and the $SNR_A$ estimator. The SAM thus appears as a valid starting signal for REB diagnostics: its spectrum is generally "cleaner" and more readable and the diagnostic information is already available without any signal processing.

## 6 Acknowledgments

The authors wish to thank the Inter Departmental Research Center INTERMECH MoRE of the University of Modena and Reggio Emilia for the financial support.

## 7 References

[1] Randall RB, Antoni J (2011) *Rolling Element Bearing Diagnostics—A Tutorial*. Mechanical Systems and Signal Processing 25: 485–520

[2] Randall RB (2011) *Vibration-based Condition Monitoring: Industrial,* Automotive and Aerospace Applications. John Wiley and Sons, West Sussex.

[3] Antoni J (2006) *The spectral Kurtosis: a useful tool for characterizing non-stationary signals*. Mechanical Systems and Signal Processing 20: 282–307

[4] Antoni J, Randall RB (2006) *The spectral Kurtosis: application to the vibratory surveillance and diagnostics of rotating machines.* Mechanical Systems and Signal Processing 20: 308–331

[5] Barszcz T, Randall RB (2009) *Application of spectral Kurtosis for detection of a tooth crack in the planetary gear of a wind turbine*. Mechanical Systems and Signal Processing 23(4): 1352–1365

[6] Cocconcelli M, Zimroz R, Rubini R, Bartelmus W (2012) *Kurtosis over Energy Distribution Approach for STFT Enhancement in Ball Bearing Diagnostics*. Proceedings of the Second International Conference "Condition Monitoring of Machinery in Non-Stationary Operations" CMMNO'2012 51-59

[7] McFadden PD, Smith JD (1984) *Vibration monitoring of rolling element bearings by the high-frequency resonance technique - a review.* Tribology International 17(1): 3-10

[8] Vrabie VD, Granjon P, Serviere C (2003) *Spectral Kurtosis: from definition to application.* IEEE-EURASIP Workshop on Nonlinear Signal and Image Processing, Grado, Italy, 2003, June 8–11.

[9] Cotogno M, Cocconcelli M, Rubini R (2013) *Spatial acceleration modulus for rolling elements bearing*. Proceedings of the Third International Conference "Condition Monitoring of Machinery in Non-Stationary Operations" CMMNO'2013.